JOURNAL OF ADVANCED MECHANICAL ENGINEERING APPLICATIONS
e-ISSN: 2716-6201

JAMEA

Vol. 6 No. 1 (2025) 1-13
https://publisher.uthm.edu.my/ojs/index.php/jamea

Investigation of the Effect of Layer Thickness and Raster Angle Orientation on the Bending Properties of Additive Manufactured Polylactic Acid (PLA) Polymer

E.K. Orhorhoro[1]*, S. Sadiq[1], E.F. Igbagbon[1], C.O. Omoyi[2]

[1] *Department of Mechanical Engineering, College of Engineering, Igbinedion University Okada, Edo State, NIGERIA*
[2] *Department of Mechanical Engineering, Faculty of Engineering, University of Calabar, Calabar, Cross River State, NIGERIA*

*Corresponding Author: ejiroghene.orhorhoro@iuokada.edu.ng
DOI: ://doi.org/10.30880/jamea.2025.06.01.001

Article Info

Received: 16 October 2024
Accepted: 17 April 2025
Available online: 30 June 2025

Keywords

3D printing, layer thickness, raster angles, bending stress, polylactic acid

Abstract

Today's mechanical engineering applications of 3D printing are highly beneficial for the study and creation of a wide range of components, from simple everyday structures to intricate ones. In fused deposition modeling, a component is usually created by applying the concepts of layer-by-layer material deposition and rapid prototyping. The effect of layer thickness and raster angle orientation on the bending characteristics of PLA beam samples that were 3D printed was examined in this work. A stereolithography (STL) file format, which was produced using modeling software (CAD), is used to transmit data into the machine's software. Three distinct raster angle orientations—0°, 45°, and 90°—as well as layer thicknesses of 0.155 mm, 0.255 mm, and 0.355 mm and 100% infill were used to print the PLA beam samples. The Instron machine was used to perform a 3-point test in order to ascertain the PLA beam samples' bending characteristics. The PLA beam sample's size and geometry were modeled using the ASTM D790-10 standard procedure. The study's findings indicate that the bending characteristics of the PLA beam samples are influenced by the layer thickness and raster angle orientation. In contrast to 45° and 90° raster angle orientation, it was found that 0° had the greatest bending effect. Additionally, in all evaluated PLA beam samples, a layer thickness of 0.355 mm yielded superior results than a layer thickness of 0.155 mm. Therefore, a raster angle of 0° and a layer thickness of 0.355 mm should be utilized when bending stress is taken into account for 3D printing PLA materials.

1. Introduction

By means of computer-aided design (CAD) data as a blueprint, additive manufacturing (AD), commonly referred to as 3D printing, is a cutting-edge fabrication technique that creates tangible objects layer by layer. In contrast to conventional subtractive manufacturing techniques, which remove material, 3D printing creates items by carefully adding material [1–5]. Complex geometries and intricate structures that may be difficult or impossible to accomplish using traditional production techniques can now be created because to this technology [6–10]. 3D printing provides design and manufacturing flexibility in a variety of industries, such as consumer products,

Nomenclature	
b	Tested beam width, mm
d	Beam depth, mm
D	Midspan deflection, mm
E_b	Modulus of elasticity in bending, MPa
L	Span support, mm,
m	The slope of the tangent to the load-deflection curve's first straight-line segment, N/mm of deflection
r	Strain
P	The load at a specific location on the load-deflection curve, N
R	Rate of the crosshead motion, mm/min,
Z	The rate of the straining of the outer fiber, mm/mm/min = 0.01
σ	The stress in the outside fibers at midpoint, MPa
ε_f	The strain in the outside surface, mm/mm,
σ_{f2} & σ_{f1}	The flexural stresses
ε_{f2} & ε_{f1}	The flexural strains

healthcare, automotive, and aerospace, by precisely depositing materials, frequently in the form of metals, polymers, ceramics, or composites [11, 12].

3D printing became a preferred tool for innovators and entrepreneurs as sectors recognized the possibilities for customisation and quick iteration. Without the need for costly tooling, it made it possible to produce prototypes, small batches, and customized goods [13]. The capabilities of 3D printing were increased by the creation of new materials. Environmentally minded enterprises took notice of the technique since it could create intricate geometries with little waste [14]. Advances in technology and ongoing study are pushing the limits of 3D printing. Improved surface finishes, increased build volumes, faster printing rates, and advancements in multi-material printing are all examples of this [15]. Overall, 3D printing's revolutionary capabilities—from rapid prototyping to the fabrication of end-use parts—have increased its acceptability. 3D printing is probably going to continue to be a hot topic for attention and expansion in advanced manufacturing and design as usage spreads throughout industries and new, creative uses appear. 3D printing is a rapid manufacturing process that uses digital models to accomplish three-dimensional product superposition forming and automatically controlled nozzles [16–18]. The benefits of 3D printing over traditional production include a shorter printing cycle and a printable composite model [19, 20]. Rapid prototyping technologies can help reduce the time and processes involved in the process, which is the general goal of 3D printing. In order to produce the design and, consequently, the product in the shortest amount of time, the AM employs 3D modelling software such as CAD [21, 22]. Using the information from the design program, the product is made by layering consecutive layers of material on top of one another [23–25]. Single step manufacturing (SSM) and multi-step manufacturing (MSM) are the two main categories into which 3D printing technology falls [26]. As the name suggests, a single step uses material fusion [27] to achieve the basic geometry, whereas a multi-step procedure uses the adhesion principle to achieve the basic geometry and is carried out in several steps. Fused Deposition Modelling (FDM), Laminated Object Manufacturing (LOM), Selected Laser Melting (SLM), Stereolithography, and Selective Laser Sintering are some of the different 3D technological methods [28–30]. Fused deposition molding (FDM) technique has been the most widely used 3D printing method due to its low cost and ease of equipment operation [31–35]. In addition to being the fastest and easiest to use, this technique is regarded as one of the most significant and basic AM technologies [36–38].

Polymers are materials that are widely utilized in 3D printing as a result of their flexibility [39], cost [40], and convenience of usage [41]. They are made up of materials including polymers, resins, and rubber-like compounds that may be melted and extruded into various shapes [42]. Polymers of several types, each with unique properties and uses, are employed in 3D printing. Polylactic acid (PLA), one of the most widely used polymer materials, is projected to dominate the desktop 3D printing market [43]. Prototyping, models, do-it-yourself projects, creative things, home goods, low-wear toys, packaging, and biomedical applications are among the applications of PLA in 3D printing [44]. It has many benefits, including easy printing, a large range of colors and designs, and—above all—biodegradability [45]. Due to its low melting point, lack of toxicity, lack of irritation, and biocompatibility, PLA is the most important material for 3D printing and is widely used in FDM technology [46]. However, the material used in 3D printing has not been widely used as a primary load-bearing structure. This is because the

Int. Journal of Integrated Engineering Vol. 6 No. 1 (2025) p. 1-13

mechanical properties of the samples during the 3D printing forming process are greatly influenced by process parameters like printing temperature, raster angle orientation, speed, and layer thickness [47]. As a result, its mechanical qualities fall short of expectations [48]. Even if there have been some studies in that field, much more work has to be done. [49] used digital image correlation (DIC) to examine the mechanical characteristics of PLA lattice structures that were 3D printed. They also assessed how process parameters affected the samples' mechanical characteristics. [50] created thermoplastic composite materials bonded with carbon fiber using FDM. They examined the effects of carbon fiber length and content on the sample's mechanical behavior, as well as bending performance, which includes bending stress, flexural modulus, flexural toughness, and flexural yield strength as the testing index. Tensile strength, young's modulus, toughness, and yield strength were grouped as tensile properties. Accordingly, [51] created PLA and continuous fiber samples using FDM and investigated how process variables affected the mechanical characteristics of printed composite materials. The continuous fiber reinforced composite FDM was printed with a corrugated structure, yielding a maximum compressive strength of 17.17 MPa and a fiber content of 11.5% [52]. [53] examined the connection between process characteristics and failure mode under compression load. They used electron beam melting and selective laser melting (SLM) to create lattice structures using various process parameters. [54] prepared continuous fiber reinforced thermosetting composite samples using FDM in order to characterize its mechanical properties. According to their research, thermosetting composites have superior mechanical qualities than the same type of thermoplastic materials. Additionally, six polymer lattice structures with various cell topologies were printed and their quasi-static energy absorption impact was investigated [55]. The results of the investigation demonstrated that the dominating structure for tensile buckling was stronger and more rigid, with a smaller energy absorption effect. [36,37] used numerical simulation and experimentation to examine the effects of four different kinds of vertical braced element architectures on the element stiffness, failure load, and sea efficiency. Additionally, [56] looked into the mechanical characteristics of 3D printed polymer structures and the compressive qualities of honeycomb structures reinforced by hollow trusses. [57] printed the samples at 0°, 45°, and 90° orientations to examine their impact on the sample's mechanical characteristics. The results of the previously described investigations demonstrated that 102 MPa was the maximum bending stress generated at a raster angle of 0°. Although there is documentation of the mechanical behaviors of 3D printed materials, the majority of these studies do not determine the optimal and lowest printing layer thickness and raster angle orientation that could enhance PLA materials' optimum bending capabilities. Thus, this work aims to investigate the effects of raster angle and layer thickness on the bending properties of PLA material. Three different printed layer thicknesses with raster angle orientations of 0°, 45°, and 90° are utilized to evaluate the bending properties of a PLA beam sample.

2. Materials and Methods

The ANSYS Workbench Package was used to model the PLA material beam, specifically the Space Claim software that comes with this software package. In the ANSYS program, the Space Claim makes it possible to create geometries that can be utilized in subsequent simulations. Microsoft Windows can run Space Claim, a solid modeling computer-aided design (CAD) program. Because the ANSYS Space Claim application is simple, anyone can create, modify, and fix geometry with ease without interfering with the underlying technology. Fig. 1 displays the PLA sample beam's dimensions. The model that was equally modeled on Autodesk Inventor was used to create the STL file. In order to facilitate the additive manufacture of the samples, this software made it possible to create an STL file that could be easily entered into the Fused Deposition Modelling (FDM) 3D printer.

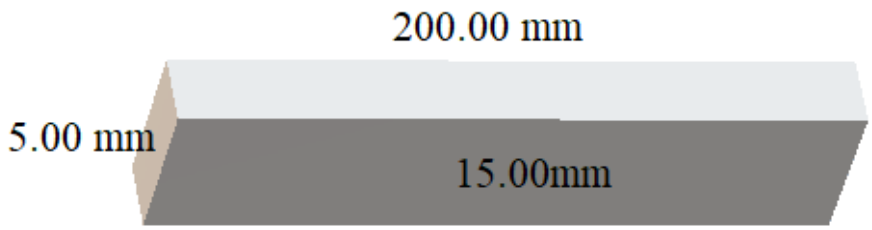

Fig. 1 Creating the PLA sample for 3D printer

The FDM 3D printer uses additive manufacturing techniques to create 3D PLA beam samples. The build volume of the FDM 3D printer is 254 mm in width, 254 mm in length, and 254 mm in height. It can be applied to items with tighter tolerances that are bigger and more intricate. Using a heated nozzle, the 3D printer extrudes PLA beam filament, which is then deposited onto a build platform. The printed PLA beam samples are included in the print for accuracy purposes and are created during file processing using ANSYS. Table 1 displays the details of the test PLA beam sample, and Table 2 displays the test information. The schematic diagram of the PLA beam samples raster angles orientation (0^0, 45° and 90°) is shown in Fig. 2.

Table 1 *Details of PLA beam samples*

Number of Tests	Layer Orientation	Layer Thickness (mm)	Sample Infill (%)	Sample Width (mm)	Sample Height (mm)
		Sample 1			
Test i	0^0	0.355	100	15.00	5.00
Test ii	0^0	0.355	100	15.00	5.00
Test iii	0^0	0.355	100	15.00	5.00
		Sample 2			
Test i	45^0	0.355	100	15.00	5.00
Test ii	45^0	0.355	100	15.00	5.00
Test iii	45^0	0.355	100	15.00	5.00
		Sample 3			
Test i	90^0	0.355	100	15.00	5.00
Test ii	90^0	0.355	100	15.00	5.00
Test iii	90^0	0.355	100	15.00	5.00
		Sample 4			
Test i	0^0	0.255	100	15.00	5.00
Test ii	0^0	0.255	100	15.00	5.00
Test iii	0^0	0.255	100	15.00	5.00
		Sample 5			
Test i	45^0	0.255	100	15.00	5.00
Test ii	45^0	0.255	100	15.00	5.00
Test iii	45^0	0.255	100	15.00	5.00
		Sample 6			
Test i	90^0	0.255	100	15.00	5.00
Test ii	90^0	0.255	100	15.00	5.00
Test iii	90^0	0.255	100	15.00	5.00
		Sample 7			
Test i	0^0	0.155	100	15.00	5.00
Test ii	0^0	0.155	100	15.00	5.00
Test iii	0^0	0.155		15.00	5.00
		Sample 8			
Test i	45^0	0.155	100	15.00	5.00
Test ii	45^0	0.155	100	15.00	5.00
Test iii	45^0	0.155	100	15.00	5.00
		Sample 9			
9 Test i	90^0	0.155	100	15.00	5.00
Test ii	90^0	0.155	100	15.00	5.00
Test iii	90^0	0.155	100	15.00	5.00

Table 2 *Details of 3D bending test*

S/N	Requirement	Details
1	Testing Machine	100kN Instron machine
2	Test Frame Model	5985
3	Load Measurement Accuracy	±0.5%
4	Test Loading Rate	2.70 mm/min
5	Testing Software	Instron Bluehill Universal
6	Distance Between Lower Anvils	90 mm
7	Anvil Radii (Upper & Lower)	5 mm

Int. Journal of Integrated Engineering Vol. 6 No. 1 (2025) p. 1-13

a. Schematic diagram of PLA Beam Samples Raster Angles Orientation (0^0, 45° and 90°)

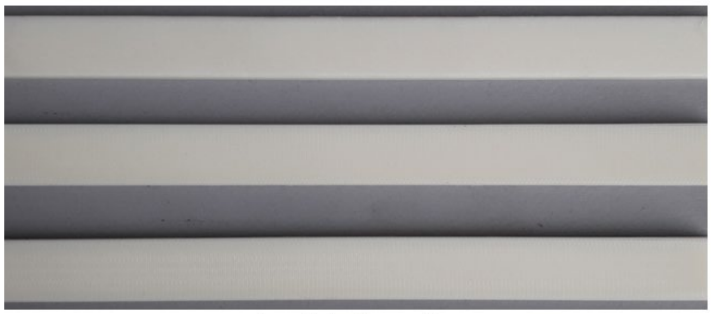

b. Actual samples

Fig, 2 *PLA beam samples raster*

The PLA beam samples are printed with a thickness layer of 0.355 mm, 0.255 mm, and 0.155 mm with 100% infill in three distinct raster angle orientations (0°), 45°, and (90°) for the bending stress test analysis. For every sample collection, three PLA beams were manufactured using an FDM 3D printer, and each one underwent 3-point flexural testing with an Instron testing apparatus. The test PLA beam samples' dimensions and geometry were created using ASTM D790-10 standard test procedures for electrical insulating materials and the bending characteristics of reinforced and unreinforced plastics. The rectangular cross-section PLA beam samples were loaded using a loading nose positioned halfway between the supports after being supported by two supports. Additionally, in use are a strain rate of 0.01 mm/mm/min and a support span-to-depth ratio of 16:1. The depth of the PLA beam samples was thus 16 times the support span. The machine's crosshead motion rate is determined by applying eqn (1).

$$R = \frac{ZL^2}{6d} \tag{1}$$

Eqn (2) is used to calculate the deflection at which this strain will occur by letting r equal 0.05 mm/mm.

$$D = \frac{rL^2}{6d} \tag{2}$$

Eqn (3) is used to calculate the PLA beam sample's flexural stress (σ_f) when it is supported at two locations and loaded at the middle, and eqn (4) is used to calculate the flexural strain (ε_f) for any deflection.

$$\sigma_f = \frac{3PL}{2bd^2} \tag{3}$$

$$\varepsilon_f = \frac{6Dd}{L^2} \tag{4}$$

Eqn (5) is used to determine the tangent modulus of elasticity. Chord modulus was calculated from two different places on the load deflection curve, and it was assessed by drawing a tangent to the steepest starting straight-line segment of the load-deflection curve. Eqn (6) was used to compute the chord modulus.

$$E_B = \frac{L^3 m}{4bd^3} \tag{5}$$

$$E_f = \frac{\sigma_{f2} - \sigma_{f1}}{\varepsilon_{f2} - \varepsilon_{f1}} \tag{6}$$

Where b represent the tested beam width measured in mm; d implies the depth of the beam in mm; D indicates the midspan deflection measured in mm; E_B means the modulus of elasticity obtained during bending (MPa); L

indicates the span support in mm; m represent the slope of the tangent to the initial straight-line portion of the load-deflection curve measured in N/mm of deflection; r = implies the strain; while P represent the load at a given point on the load-deflection curve measured in N. Also, R indicates the rate of crosshead motion (mm/min); Z represent the rate of straining of the outside fiber; σ suggests the stress in the outside fibers at midpoint (MPa); ε_f indicates the strain in the outside surface (mm/mm); σ_{f2} and σ_{f1} indicates the flexural stresses; and ε_{f2} and ε_{f1} represent the flexural strains

3. Results and Discussion

The force-displacement and stress/strain curves were plotted using the force-displacement data from the three-point bending test. The results of force/displacement analysis of different layer thickness and at different raster angle orientation FDM 3D printing of PLA beam samples is shown in Fig. 3 to Fig. 5. A layer thickness of 0.355 mm was found to have superior plastic deformation, as indicated by the displacement/force curve (Fig. 3-5). In contrast to a layer thickness of 0.155 mm, which yields an ultimate force of 158 N, a layer thickness of 0.355 mm provides an ultimate force of 165 N prior to failure.

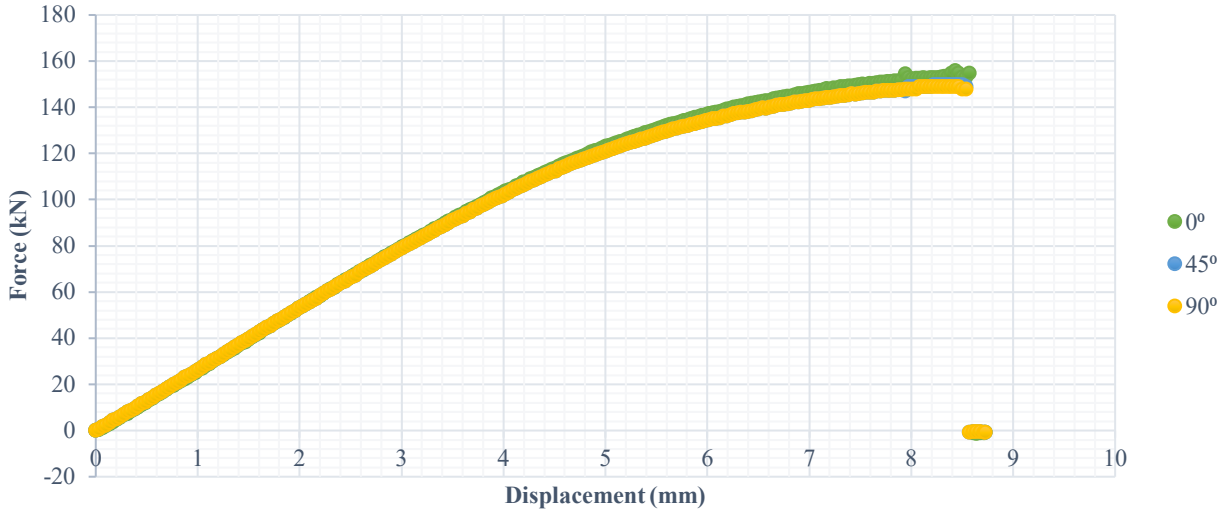

Fig. 3 *Graph of force against displacement for print layer thickness of 0.155 mm at raster angle orientation of 0°, 45^0, & 90^0*

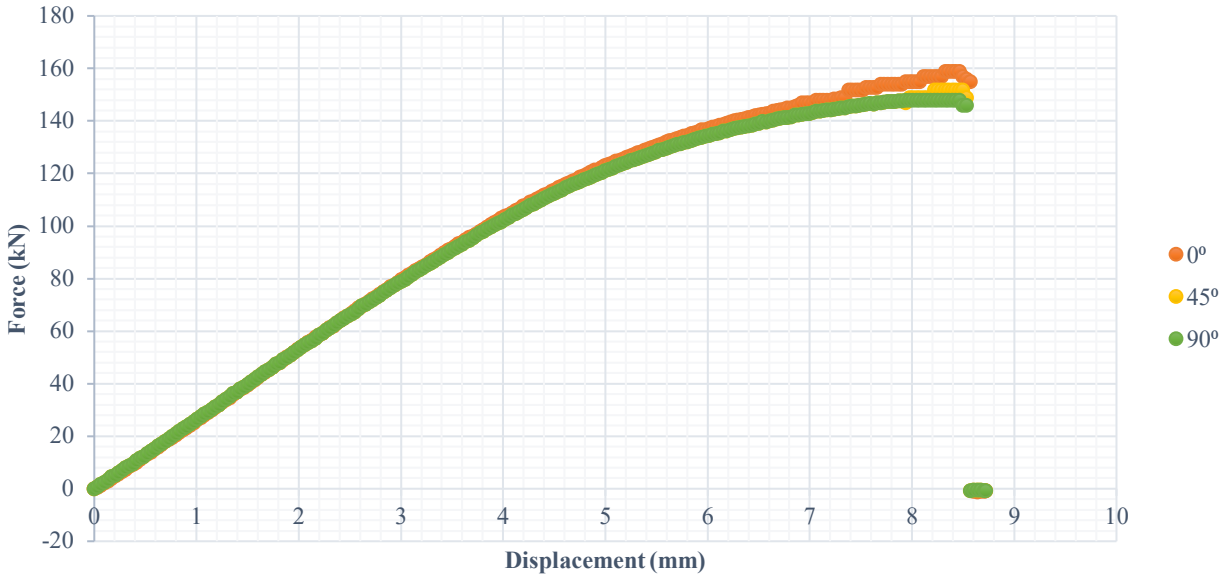

Fig. 4 *Graph of force against displacement for printed layer thickness of 0.255 mm at raster angle orientation of 0°, 45^0, & 90^0*

Int. Journal of Integrated Engineering Vol. 6 No. 1 (2025) p. 1-13

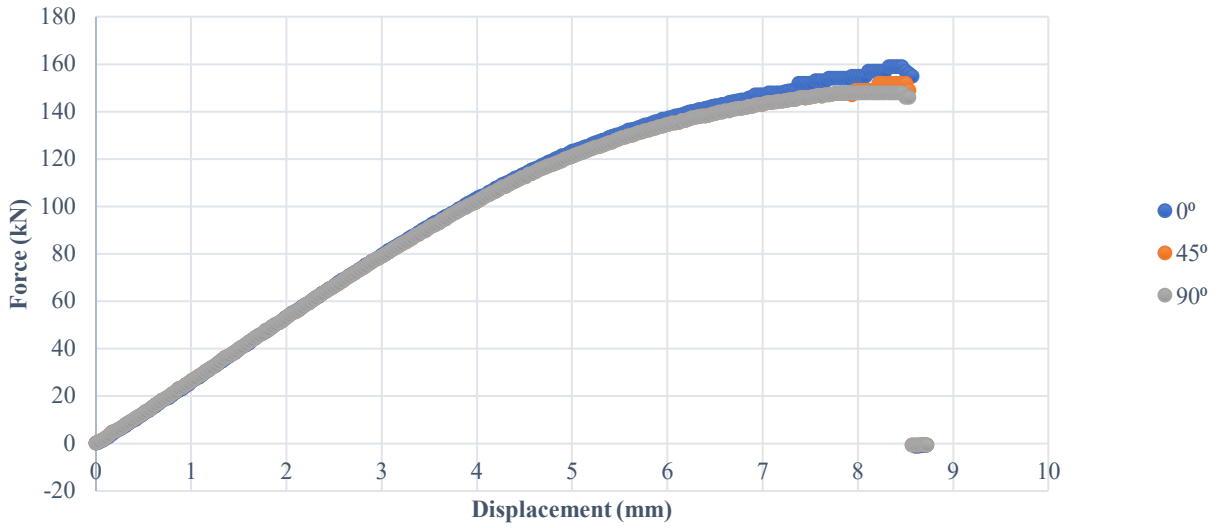

Fig. 5 *Graph of force against displacement for printed layer thickness of 0.355 mm at raster angle orientation of 0°, 45^0, & 90^0*

Figs. 6 and 8 display the stress/strain curve's findings. The bending characteristics of the PLA beam samples were significantly impacted by the layer thickness. The PLA beam samples' stress behavior was impacted by variations in layer thickness. Better stress-strain behavior was found with a printed layer thickness of 0.355 mm. In contrast to a layer thickness of 0.155 mm, which results in an ultimate stress of 1.8 MN/m2 (Fig. 6), a layer thickness of 0.355 mm yields an ultimate stress of 2.25 MN/m^2 (Fig. 8) prior to failure. Therefore, the bending behavior of the PLA beam samples employed in this investigation increased in proportion to an increase in layer thickness from 0.155 to 0.355 mm. The findings are comparable to the research on the impact of layer thickness on the fatigue mechanical behavior of PLA materials conducted by [57,58]. Additionally, according to [59], the proportion of infill is closely correlated with the quantity of material used to sustain the load. As a result, larger effective cross-section areas for load support and increased sample strength and rigidity are the results of higher infill percentages. Additionally, it was discovered that the mechanical behavior of Polyether Ether Ketone (PEEK) materials were significantly influenced by both build orientation and infill percentage. After yield, brittle fracture changed to ductile fracture, increasing strength for samples with the maximum infill percentage and build orientation in line with the loads [60]. Additionally, the bending characteristics of the PLA beam samples are influenced by the printing direction. According to the test analysis results, PLA beam samples created with a raster angle of 0o printed orientation had the maximum bending stress properties for the force/displacement curve and the stress/strain curve under the force/displacement and stress/strain curves. Furthermore, compared to PLA beam samples printed with raster angles of 0^o and 45^o, which have the highest resistance to bending, the printed PLA beam samples with a 90^o raster angle demonstrated the least amount of bending resistance. These results were comparable to those of the study conducted by [57] and [61], which investigated the impact of raster printing angles and directions on materials made of Acrylonitrile Butadiene Styrene (ABS).

A flexural stress-strain diagram, which is used to calculate flexural stress, flexural strain, tangent modulus of elasticity, and chord modulus, is used to ascertain the member's bending qualities. Flexural modulus, flexural stress and strain, modulus of elasticity in bending, and chord modulus were calculated using the stress-strain diagram, as illustrated in Figs. 9 to12. Flexural stress, chord modulus, and tangent modulus of elasticity were found to be sensitive to the orientation of the raster angle. Furthermore, the 0° raster angle orientation resulted in the highest flexural stress, whereas the 90° raster angle orientation produced the lowest. A change in raster angle from 0° to 90° similarly resulted in a drop in the tangent modulus of elasticity; the highest value recorded was 0.65MN/m^2 for raster angle orientation of 0° and layer thickness of 0.3555 mm. With a 90° raster angle orientation and a 0.155 mm layer thickness, the lowest value, however, is 0.50 MN/m^2. However, for the chord modulus, the 90° raster angle orientation had the maximum value of 1.23 MN/m^2 for printed layer thickness of 0.355 mm. This was not the case for the bending stress, flexural strain, and tangent modulus of elasticity, where the 0° raster angle orientation has the maximum value. Therefore, the bending stress in the PLA beam samples will be reduced by raising their chord modulus. The bending stress may have decreased as a result of a decrease in distance from the neutral axis and an increase in moment of inertia [58,59]. Additionally, the midspan deflection and test loading rate were measured at 10.67 mm and 2.70 mm/min, respectively.

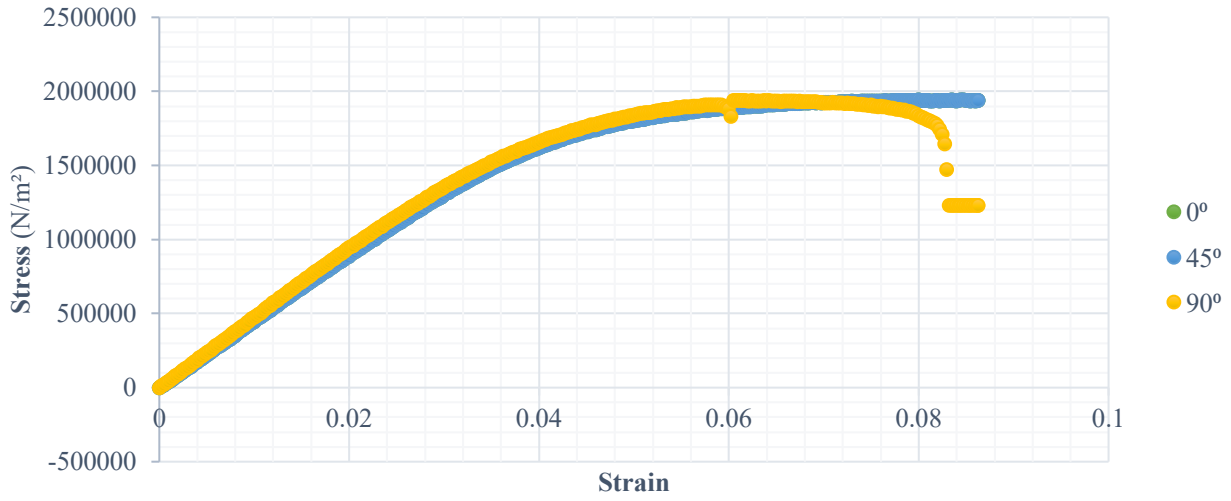

Fig. 6 *Graph of stress against strain for print layer thickness of 0.155 mm at raster angle orientation of 0°, 45⁰, & 90⁰*

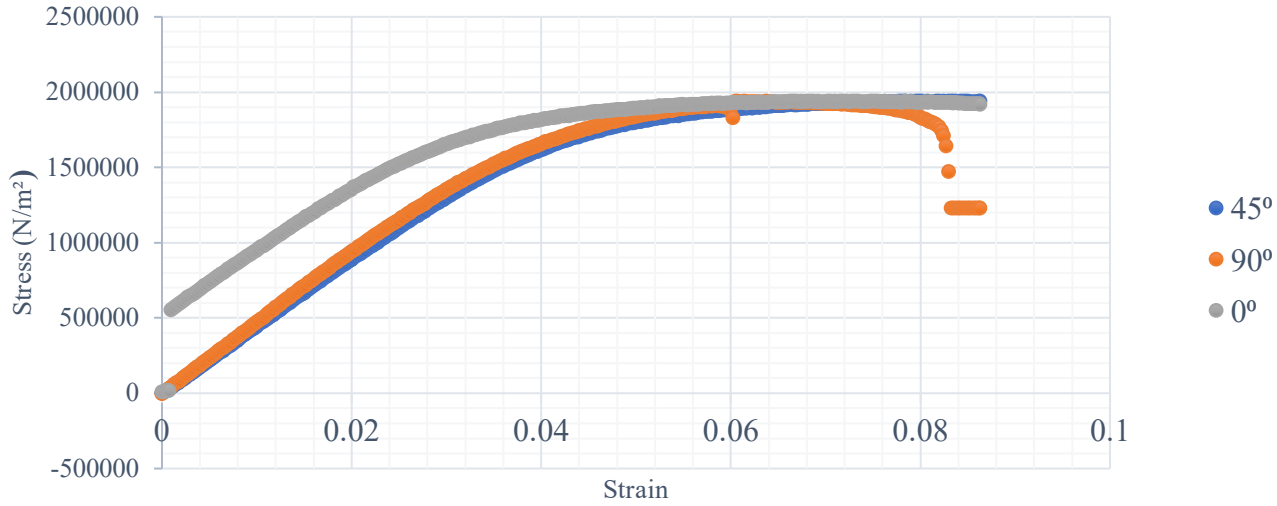

Fig. 7 *Graph of stress against strain for print layer thickness of 0.255 mm at raster angle orientation of 0°, 45⁰, & 90⁰*

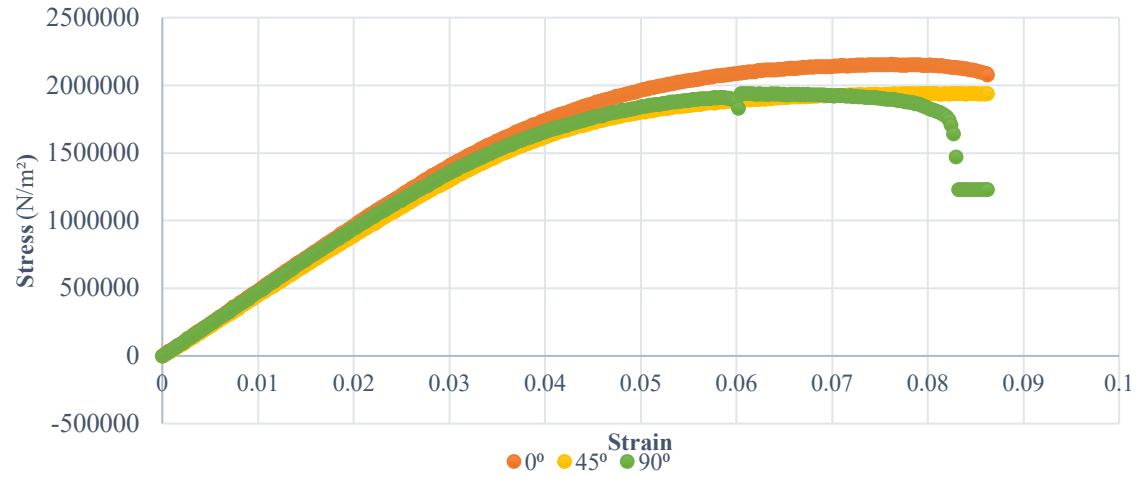

Fig. 8 *Graph of stress against strain for print layer thickness of 0.355 mm at raster angle orientation of 0°, 45⁰, & 90⁰*

Int. Journal of Integrated Engineering Vol. 6 No. 1 (2025) p. 1-13

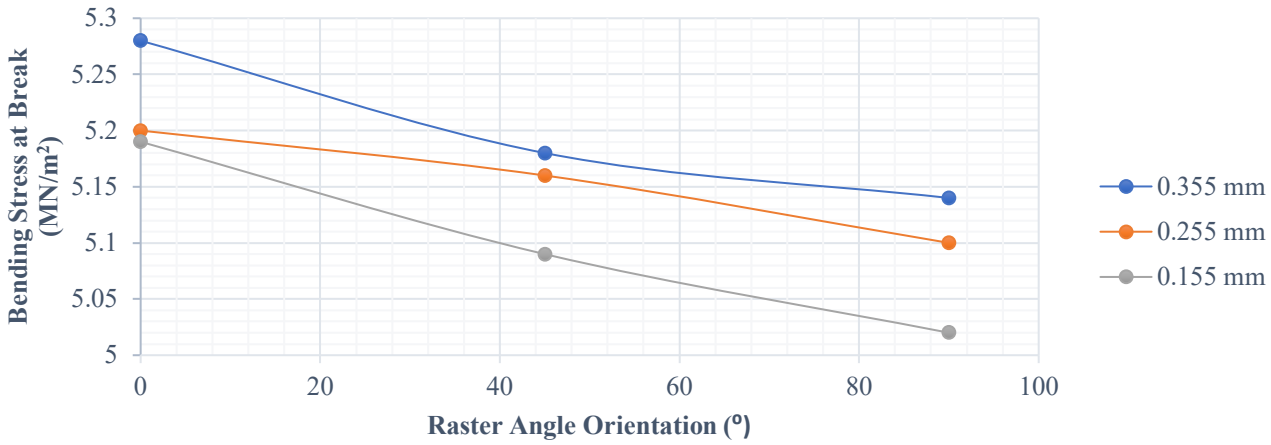

Fig. 9 *Evaluation of bending stress at break*

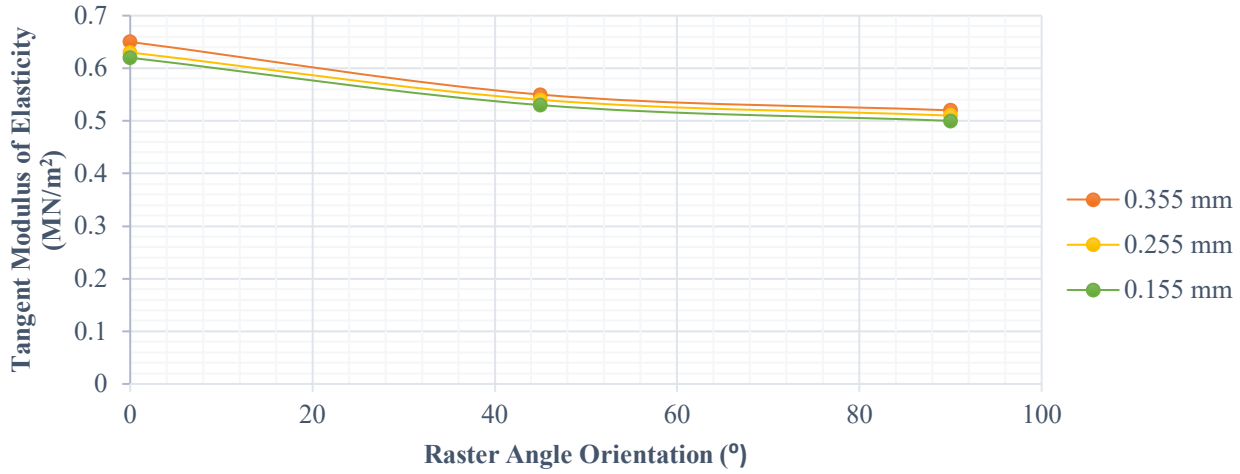

Fig. 10 *Evaluation of tangent modulus of elasticity*

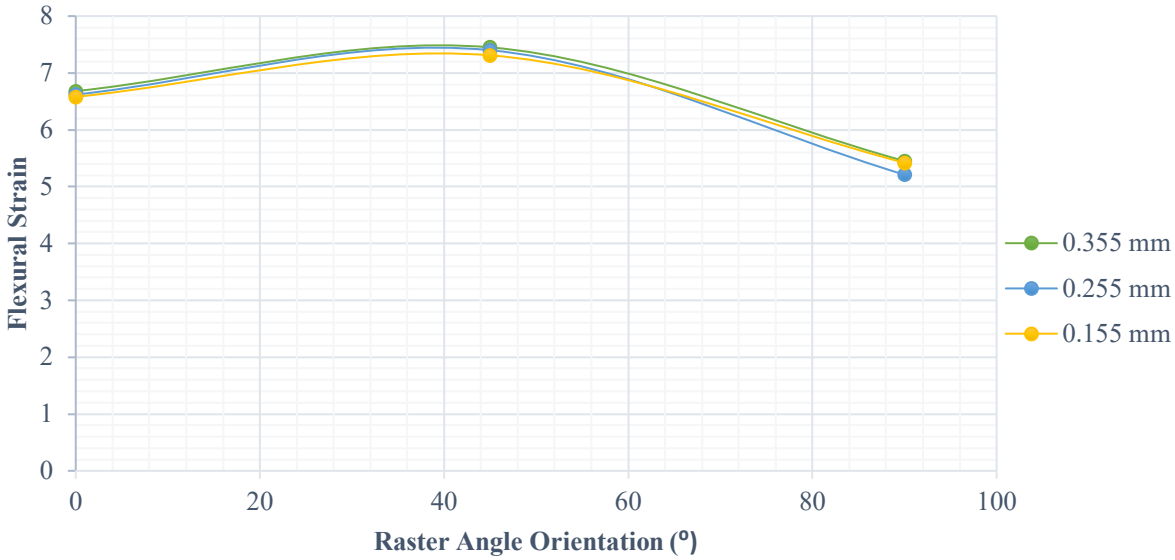

Fig. 10 *Evaluation of flexural strain*

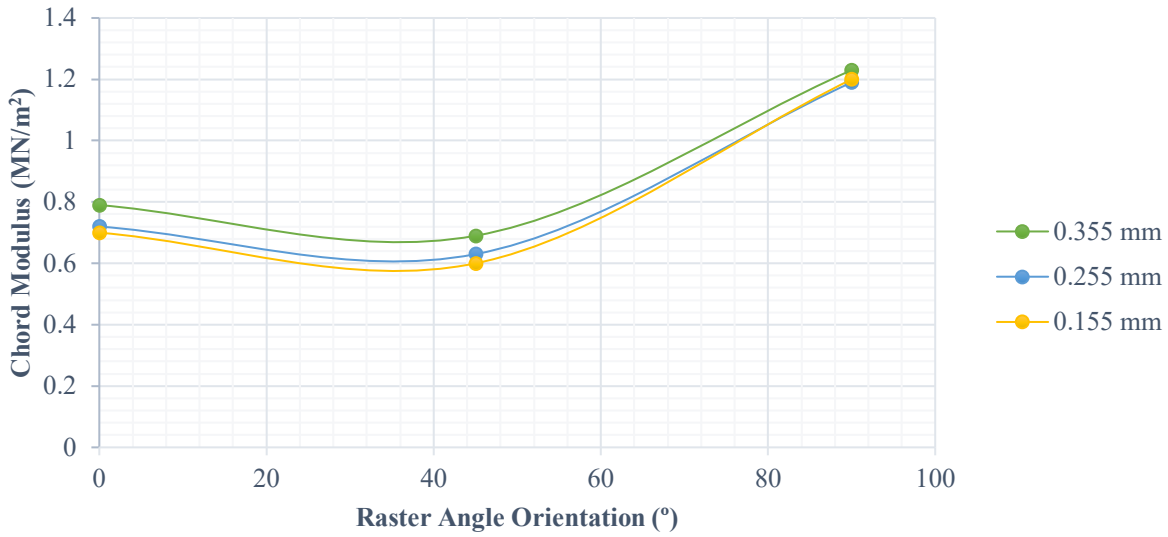

Fig. 11 *Evaluation of chord modulus*

4. Conclusion

In this study, a 3D printed PLA beam samples were evaluated for mechanical bending stress analysis. An effective 3-point-pointing test was performed on PLA beam samples that were 3D printed. The flexural stiffness of the beam samples was determined using the force against displacement data. The flexural characteristics of the beams were obtained by converting the force-displacement data into stress-strain data. Three PLA beam samples are printed in each set of 0°, 45°, and 90° at varying layer thicknesses of 0.355 mm, 0.255 mm, and 0.155 mm in order to ensure precise results. The bending qualities of PLA beam samples are significantly impacted by layer thickness and raster angle orientation, according to testing of bending samples. Additionally, at a layer thickness of 0.355 mm, the 0° raster orientation has the highest force of 165 N, while 45° and 90° have forces of 155 N and 150 N, respectively. Additionally, the 0° raster angle orientation and layer thickness of 0.355 mm were used to determine the maximum flexural stress at break value, which is 5.28 MN/m^2. Additionally, for raster angle orientations of 0-90°, the tangent modulus of elasticity results in a reduction in flexural stress. However, because the raster angle of 90° orientation has a maximum value of 1.23 MN/m^2 for layer thickness of 0.355 mm, the chord modulus exhibits a distinct trend. According to this study, the bending behavior of PLA materials produced by additive manufacturing is influenced by the thickness layer and printing orientation angles. The study further proves that irrespective of the layer thickness, printing at raster angle orientation of 0^0 produced the most favourable bending properties such as bending stress, tensile strength, and fatigue strength. Similarly, in printing in the range of the layer thickness from 0-0.355 mm, printing at layer thickness of 0.355 mm will produce optimum values that will favour bending properties of PLA materials.

Acknowledgement

We are grateful to everyone and institution we have collaborated with: College of Engineering workshop, Igbinedion University Okada, University of Benin Energy Research Centre, Defence Research and Development Bureau Nigeria, Abuja, and Petroleum Training Institute, Effurun, Delta State, Nigeria.

Conflict of Interest

Regarding the paper's publication, the authors affirm that they have no conflicts of interest.

Author Contribution

Ejiroghene Kelly Orhorhoro conducted the ***feasibility study, analyzed the results and overseen the study****. Sadiq Sule took part in the* ***experiment, test analysis, and the study conceptual framework and results documentations****. Efe Justic Igbagbon took part in* ***literature review and results interpretation****, and Cordelia Ochuole Omoyi* ***reviewed the study*** *prior to submission.*

References

[1] Shergill, K., & Chen, S.B. (2023) What controls layer thickness effects on the mechanical properties of additive manufactured polymers, *Surface & Coatings Technology,* 475, 130131. https://doi.org/10.1016/j.surfcoat.2023.130131

[2] Manoj Prabhakar, M., Saravanan, A.K., Haiter Lenin, A., Jerin Leno, I., Mayandi, I., Sethu Ramalingam, P. (2021) A short review on 3D printing methods, process parameters and materials, *Mater. Today Proc.,* 45, 6108–6114

[3] Gonabadi, H., Yadav, A., & Bull, S.J. (2020) The effect of processing parameters on the mechanical characteristics of PLA produced by a 3D FFF printer, *Int. J. Adv. Manuf. Technol.,* 111, 695–709

[4] Gonabadi, H., Chen, Y., Yadav, A., Bull, S.J. (2022) Investigation of the effect of raster angle, build orientation and infill density on the elastic response of 3D printed parts using Finite Element microstructural modelling and homogenization techniques, *Int. J. Adv. Manuf. Technol.,* 118, 1485–1510.

[5] Hsueh, M., Lai, C., Wang, S., Zeng, Y., Hsieh, C., Pan, C., Huang, W. (2021) Effect of printing parameters on the thermal and mechanical properties of 3D-printed PLA and PETG, using fused deposition modelling, *Polymers*, 13(11), 1758

[6] Syrlybayev, D., Zharylkassyn, B., Seisekulova, A., Akhmetov, M., Perveen, A., Talamona, D. (2021) Optimisation of strength properties of FDM printed parts—a critical review, *Polymers,* 13(10), 1587

[7] Sharma, M., Sharma, V., Kala, P. (2019) Optimization of process variables to improve the mechanical properties of FDM structures, J. *Phys. Conf. Ser.,* 1240, 012061

[8] Kristiawan, R.B., Imaduddin, F., Ariawan, D., Ubaidillah, A.Z. (2021) A review on the fused deposition modeling (FDM) 3DP: filament processing, materials, and printing parameters, *Open Eng.,* 11, 639‑649. https://doi.org/10.1515/eng-2021-0063

[9] Dhinesh, S.K., Arun, P.S., Senthil, K.K.L., Megalingam, A. (2021) Study on flexural and tensile behavior of PLA, ABS and PLAABS materials, *Mater Today Proc.,* 45, 1175‑1180. https://doi.org/10. 1016/j.matpr. 2020.03.546

[10] Samykano, M., Selvamani, S., Kadirgama, K., Ngui, W., Kanagaraj, G., Sudhakar, K. (2019) Mechanical property of FDM printed ABS: influence of printing parameters, *Int. J. Adv. Manuf. Technol.,* 102 (9–12), 2779–2796.

[11] Ilyas, R.A., Sapuan, S.M., Kadier, A., Kalil, M.S., Ibrahim, R., Atikah, M.S., Nurazzi, N.M., Nazrin, A., Lee, C.H., Norrrahim, M.N., & Sari, N.H. (2021) Properties and characterization of PLA, PHA, and other types of biopolymer composites, *In: Advanced processing, properties, and applications of starch and other bio-based polymers*, 111‑138

[12] Liao, L., Liu, C., Coppola, B., Barra, G., Di Maio, L. Incarnato, L., & Lafdi, K. (2019) Effect of porosity and crystallinity on 3D printed PLA properties, *Polymers,* 11, 1487. https://doi.org/10.3390/polym11091487

[13] Baran, E.H., & Erbil, H.Y. (2019) Surface Modification of 3D printed PLA objects by fused deposition modeling: a review, *Colloids Interfaces,* 3, 43. https://doi.org/10.3390/collo ids3020043

[14] Van den Eynde, M., Van Puyvelde, P. (2018) 3DP of poly(lacticacid). In: Di Lorenzo ML, Androsch R (Eds.). Ind Appl PLA, *Springer International Publishing, Cham,* 139‑158. https://doi.org/10.1007/12201728

[15] Vicente, C., Martins, V., Leite, M., Ribeiro, A., & Reis L. (2019) Influence of fused deposition modeling parameters on the mechanical properties of ABS parts, *Polym. Adv. Technol.,* 31 (3), 501–507

[16] Liao, G., Li, Z., Cheng, Y., Xu, D., Zhu, D., Jiang, S., Guo, J., Chen, X., Xu, G., & Zhu, Y. (2018) Properties of oriented carbon fiber/polyamide 12 composite parts fabricated by fused deposition modeling, *Mater. Des.,* 139, 283–292

[17] Chohan, J.S., Singh, R., Boparai, K.S., Penna, R., Fraternali, F. (2017) Dimensional accuracy analysis of coupled fused deposition modeling and vapour smoothing operations for biomedical applications, *Compos. Part B Eng.,* 117, 138-149

[18] Sodeifian, G., Ghaseminejad, S., Yousefi, A.A. (2019) Preparation of polypropylene/short glass fiber composite as Fused Deposition Modeling (FDM) filament, *Results Phys.,* 12, 205–222

[19] Jatti, AV., Jatti, A., Patel, V., & Jatti, V. (2019) A study on effect of fused deposition modelling process parameters on mechanical properties, *Int. J. Sci. Technol. Res.,* 8 (11), 689–693

[20] Alafaghani, A., Qattawi, A., Alrawi, B., & Guzman, A. (2017) Experimental optimization of fused deposition modelling processing parameters: a design-for-manufacturing approach, *Procedia Manuf.,* 10, 791–803

[21] Aziz, R., Haq, M.I.U., & Raina, A. (2020) Effect of surface texturing on friction behaviour of 3D printed polylactic acid (PLA), *Polym. Test.,* 85, 106434

[22] Chadha, A., Haq, M.I.U., Raina, A., Singh, R.R.R., Penumarti, N.B., Bishnoi, M.S. (2019) Effect of fused deposition modelling process parameters on mechanical properties of 3D printed parts, *World J. Eng.,* 16 (4), 550-559

[23] Ashrafi, N., Duarte, J.P., Nazarian, S., & Meisel, N.A. (2019) Evaluating the relationship between deposition and layer quality in large-scale additive manufacturing of concrete, *Virtual Phys. Prototyp.,* 14 (2), 135-140

[24] Naveed, N. (2020) Investigate the effects of process parameters on material properties and microstructural changes of 3D-printed specimens using fused deposition modelling (FDM), *Mater. Technol.,* 1-14

[25] Naveed, N. (2021) Investigating the material properties and microstructural changes of fused filament fabricated PLA and tough-PLA parts, *Polymers,* 13 (9), 1487

[26] Kumar, K.P.A., Ghosh, K., Alduhaish, O., Pumera, M. (2020) Metal-plated 3D-printed electrode for electrochemical detection of carbohydrates, *Electrochem. Commun.,* 120, 106827

[27] Farashi, S., & Vafaee, F. (2022) Effect of printing parameters on the tensile strength of FDM 3D samples: a meta-analysis focusing on layer thickness and sample orientation, *Prog. Addit. Manuf.,* 7, 565–582

[28] Valvez, S., Silva, A.P., Reis, P.N.B. (2022) Compressive behaviour of 3D-printed PETG composites, *Aerospace,* 9 (3), 124

[29] Mushtaq, R.T., Iqbal, A., Wang, Y., Khan, A.M., Abu Bakar, M.S. (2023) Parametric optimization of 3D printing process hybridized with laser-polished PETG polymer, *Polym. Test.,* 125, 108129

[30] Zhang, R., Li, L., Long, S., Wang, P., Wen, F., Yang, J., & Wang, G. (2022) High-temperature dielectric polymer composite films of all-organic PVDF/ABS with excellent energy storage performance and stability, *J. Mater. Chem. C*., 10 (9), 3480–3488.

[31] Li, G., Zhao, M., Xu, F., Yang, B., Li, X., Meng, X., Teng, L., Sun, F., Li, Y. (2020) Synthesis and biological application of polylactic acid, *Molecules,* 25(21), 5023

[32] P´eter, T., Litauszki, K., & Kmetty, A. (2021) Improving the heat deflection temperature of poly (lactic acid) foams by annealing, *Polym. Degrad. Stab.,*190, 109646

[33] Sewiko, R., Hakim, M.R., Firdaus, A.N., Alfaris, L., Baswantara, A., Wibowo, Y.A., & Krisnafi, Y. (2019) Use of acrylonitrile butadiene styrene and polylactide filaments as basic materials for marine technology prototype, *Int. J. Eng. Sci. (IJES),* 8, 75–82

[34] Nguyen, H.T.H., Qi, P., Rostagno, M., Feteha, A., & Miller, S.A. (2020) The quest for high glass transition temperature bioplastics, *J. Mater. Chem. A.,* 6(20), 9298–9331

[35] Hapo´nska, M., Clavero, E., Salvad´o, J., & Torras C. (2018) Application of ABS membranes in dynamic filtration for Chlorella sorokiniana dewatering, *Biomass Bioenergy,* 111, 224–231

[36] Fadeel, A., Mian, A., Al Rifaie, M., & Srinivasan, R. (2019) Effect of vertical strut arrangements on compression characteristics of 3D printed polymer lattice structures: experimental and computational study, *J. Mater. Eng. Perform.,* 28, 709–716

[37] Zhao, Y., Zhao, K., Li, Y., & Chen, F. (2020) Mechanical characterization of biocompatible PEEK by FDM*., J. Manuf. Process.,* 56, 28-42, 10.1016/j.jmapro.2020.04.063

[38] Zhao, G., Wang, B., Hou, H., Hao, W., & Luo, Y. (2020) Improving the interlaminar fracture toughness of carbon fiber/epoxy composites using clustered microcapsules, *Polym. Test,* 87, 106562

[39] Mercado-Colmenero, J.M., La Rubia, M.D., Mata-Garcia, E., Rodriguez-Santiago, M., & Martin-Do˜nate, C. (2022) Experimental and numerical analysis for the mechanical characterization of PETG polymers manufactured with FDM technology under pure uniaxial compression stress states for architectural applications, *Polymers,* 12(10), 2020, 2202

[40] Shi, Q., Xiao, R., Yang, H., Li Min Dong, H. (2019) Effects of physical aging on thermomechanical behaviors of poly (ethylene terephthalate)-glycol (PETG), *Polym. Plast. Technol. Mater.,* 59(8), 835–846

[41] Casavola, C., Cazzato, A., Moramarco, V., & Renna, G. (2019) Mechanical behaviour of ABS-fused filament fabrication compounds under impact tensile loadings, *Materials,* 12(8), 1295

[42] Orhorhoro, E.K., Emifoniye, E.U., Okuma, S.O. (2023) Prediction of the Tensile Strength of an Experimental Design Reinforce Polyvinyl Chloride Composite using Response Surface Methodology, *Jordan Journal of Mechanical and Industrial Engineering,*17(3), 403– 412 https://doi.org/10.59038/jjmie/170309

[43] Rahim, T.N.A.T., Abdullah, A.M., Md Akil, H. (2019) Recent developments in fused deposition modeling-based 3D printing of polymers and their composites, *Polym. Rev.,* 59 (4), 2019, 589–624

[44] Abdelaziz, A.M., Dacrory, S., Hashem, A.H., Attia, M.S., Hasanin, M., Fouda, M.H., Kamel, S., & ElSaied, H. (2021) Protective role of zinc oxide nanoparticles-based hydrogel against wilt disease of pepper plant, *Biocatal Agric Biotechnol,* 35, 102083. https://doi.org/10.1016/j.bcab.2021.102083

[45] Joseph, T.M., Kallingal, A., Suresh, A.M., Mahapatra, D.K., Hasanin, M.S., Thomas, J.H.S., Shokri, Z., Seidi,F., Saeb, M.R., Jin, Y., Li, C., & Xiao H. (2022) Elucidating the impact of enzymatic modifications on the structure, properties, and applications of cellulose, chitosan, starch and their derivatives: a review, *Mater Today Chem*, 24,100780. https://doi.org/10.1016/j.mtchem.2022.100780

[46] Seidi, F., Arabi Shamsabadi, A., Ebadi Amooghin, A., Saeb, M.R., Xiao, H., Jin, Y., & Rezakazemi, M. (2022) Biopolymer-based membranes from polysaccharides for CO2 separation: a review, *Environ Chem Lett.,* 20, 1083‑1128. https://doi.org/10.1007/s10311-021-01349-x

[47] Xu, J., Wu, Y., Wang, L., Li, J., Yang, Y., Tian, Y., Gong, Z., Zhang, P., & Nutt, S., & Yin, S. (2018) Compressive properties of hollow lattice truss reinforced honeycombs (Honeytubes) by additive manufacturing: Patterning and tube alignment effects, *Mater. Des.,* 156, 446–457

[48] Abueidda, D.W., Elhebeary, M., Shiang, C.A., Pang, S., Abu Al-Rub, R.K., & Jasiuk, I.M. (2019) Mechanical properties of 3D printed polymeric Gyroid cellular structures: Experimental and finite element study, *Mater. Des.,* 165, 107597

[49] Tanga, C., Liua, J., Yang, Y., Liua, Y., Jianga, S., & Hao, W. (2019) Effect of process parameters on mechanical properties of 3D printed PLA lattice structures, *Composites Part C,* 3, 100076, doi.org/10.1016/j.jcomc.2020.100076

[50] Ning, F., Cong, W., Qiu, J., Wei, J., & Wang, S. (2015) Additive manufacturing of carbon fiber reinforced thermoplastic composites using fused deposition modeling, *Compos. Part B: Eng.,* 80, 369–378

[51] Tian, X., Liu, T., Yang, C., Wang, Q., & Li D. (2016) Interface and performance of 3D printed continuous carbon fiber reinforced PLA composites, *Compos. Part A: Appl. Sci. Manuf.,* 88, 198–205

[52] Hou, Z., Tian, X., Zhang, J., & Li, D. (2018) 3D printed continuous fibre reinforced composite corrugated structure, *Compos. Struct.,* 184, 1005–1010

[53] De Pasquale, G., Luceri, F., & Riccio, M. (2019) Experimental characterization of SLM and EBM cubic lattice structures for lightweight applications, *Exp. Mech.,* 59, 469–482

[54] Hao, W., Liu, L., Zhou, H. Chen, H., & Fang, H. (2022) Preparation and characterization of 3D printed continuous carbon fiber reinforced thermosetting composites, *Polym. Test,* 65, 29–34

[55] Habib, F.N., Iovenitti, P., Masood, S.H., Nikzad, M. (2018) Fabrication of polymeric lattice structures for optimum energy absorption using Multi Jet Fusion technology, *Mater. Des.,* 155, 86–98

[56] Xu, J., Wu, Y., Wang, L., Li, K., Yang, Y., Tian, Y., Gong, Z., Zhang, P., Nutt, S. Yin, S. (2020) Compressive properties of hollow lattice truss reinforced honeycombs (Honeytubes) by additive manufacturing: Patterning and tube alignment effects, *Mater. Des.,* 156, 446–457

[57] Letcher, T., Waytashek, M. (2014) Material Property Testing of 3D-Printed Specimen in PLA on an Entry-Level 3D Printer. Proceedings of the ASME 2014 International Mechanical Engineering Congress and Exposition. Volume 2A: Advanced Manufacturing. Montreal, Quebec, Canada. November 1420, 2014, V02AT02A014. ASME. doi:10.1115/IMECE2014-39379

[58] Jerez-Mesa, J., Travieso-Rodriguez, J.A., Llum-Fuentes, J., Gomez-Gras, G., & Puig D. (2017) Fatigue lifespan study of PLA parts obtained by additive manufacturing, *Procedia Manuf.,* 13, 872-879

[59] Yang, C., Tian, Y., Li, D., Cao, Y., Zhao, F., & Shi C. (2017) Influence of thermal processing conditions in 3D printing on the crystallinity and mechanical properties of PEEK material, *J. Mater. Process Technol,* 248, 1-7, 10.1016/j.jmatprotec.2017.04.027

[60] Basgul, C., Thieringer, F.M., & Kurtz, S.M. (2021) Heat transfer-based non-isothermal healing model for the interfacial bonding strength of fused filament fabricated polyetheretherketone, *Addit. Manuf.,* 46, 102097, 10.1016/j.addma.2021.102097

[61] Azadi, M., Dadashi, A., Dezianian, S., Kianifar, M., Torkaman, S., & Chiyani, M. (2021) High-cycle bending fatigue properties of additive-manufactured ABS and PLA polymers fabricated by fused deposition modeling 3D-printing", Forces Mech 3,100016, https://doi.org/10.1016/j.finmec.2021.100016